GEOMETRIC AND DIMENSIONAL TOLERANCES APPLIED TO FREE-FORM SURFACES OF AN AIRCRAFT IN 2D TOLERANCE ANALYSIS

M. Marrocu[1], W. Polini[1], L. D'Ambrosio[2], L. Carrino[1], E. Anamateros[2]
[1]Università degli Studi di Cassino, Cassino, Italy
[2]AGUSTA Westland, Anagni, Italy

Abstract

Tolerance analysis is a critical step in designing and manufacturing of an aircraft. Huge problems may present during the assembly process if the tolerance study on a sub-component was not carried out or was ineffectual. These problems will introduce additional reworking time and product costs, which are not compatible with today's aircraft industry requirements. The approaches of the literature are not easy to apply, especially for complex aerospace assemblies, since they were born to deal with elementary features, such as plane, hole, pin and so on. So the aid of the computer is called for. Today Computer Aided Tolerancing (CAT) Softwares are readily available, but even if these tools provide good results, they have not been widely used. It may be explained by the lack of methods towards tolerancing problems.
The aim of the present paper is to present a method for tolerance analysis of an assembly involving free-form surfaces by dealing with dimensional and geometric tolerances. The case of study involves aerodynamic surfaces of flaperon. It is a structural assembly of the aircraft. It is constituted by 1 skin, 8 ribs and 1 spar. These 10 components are made in composite and are connected by adhesive. Adhesive thickness between the faced surfaces to connect should be as constant as possible in order to obtain a right structural connection. The influence of the tolerances applied to the 10 components on the value of the gap thickness at the interfaces among each couple of components has been deeply investigated by means of the proposed method.
The proposed method assists both the design and the assembly planning of complex shape components of an aircraft and constitutes a complementary technique to the current 3D tolerance analysis software packages, such as eM-Tolmate, since it is able to deal with the specificity and the complexity of an aircraft assembly.

Introduction

Concurrent Engineering is an important policy to reduce reworking times and discard products; such requirements are strongly felt in the aerospace industries. Concurrent engineering leads in a parallel way, design and manufacturing, making them communicate.

Tolerance analysis has a considerable weight in the Concurrent Engineering and represents the best way to solve assembly problems in order to ensure higher quality and lower costs. It is a critical step in designing and manufacturing of an aircraft and its importance is grown up in the last years. In fact, the need to assign dimensional and geometric tolerances to assembly components guarantees the correct working of the assembly towards structural and aerodynamic requirements. A product is designed and manufactured to perform a task and the issue of the task depends by one or more variables of the assembly that are commonly called "project functions". A project function is a variable of the assembly (commonly a dimension, a surface orientation and so on), whose value depends by the dimensions, the geometry and the tolerances assigned to the components constituting the assembly. The dimensions and the tolerances involved by the project function are called key parameters and for them the rule 70-30 is valid; i.e. 30% of the tolerances assigned to the components are responsible of the 70% of the assembly geometric variation (e.g. Ref 1). The nominal value and the tolerance range of the project function allows to guarantee the structural integrity and the aerodynamic requirements of the assembly. Practically, the dimensions and the tolerances of the assembly components combine, according with the assembly sequence, and generate the tolerance stack-up functions. Solving a tolerance stack-up function means to determine the nominal value and the tolerance range of a project function by combining the nominal values and the tolerance ranges assigned to the assembly components.
Tolerance analysis solves a linear or a no-linear tolerance stack-up function related to a project function. It may consider alternative assembly sequences in order to identify that one allowing to obtain the assembly functional requirements with the maximum value of the tolerance range assigned to the components. Huge problems may present during the assembly process if the tolerance study on a sub-component was not carried out or was ineffectual (e.g. Ref 2). It is even possible that the product design may have to be subsequently changed because of unforeseen tolerance problems not detected prior to actual assembly took place. In this case costs to the business will be high. It was estimated that 40%-60% of the production cost is due to the assembly process (e.g. Ref 3).

The study of the tolerance stack-up functions, during the design stage, is very critical for aeronautic field whereas the structures, to which high performances are required, are complex. Therefore, advanced design techniques and assembly technologies are needed.
The aim of the present work is to show a method for the tolerance analysis of an assembly involving free-form surfaces based on dimensional and geometric tolerances. The proposed method is adapt to assist both the product designer and the assembly planner to deal with complex shape assemblies belonging to an aircraft. The case of study is the part of flaperon involving aerodynamic surfaces. It is a structural component of the aircraft, that is constituted by 1 skin, 8 ribs and 1 spar, as shown in Figure 1.

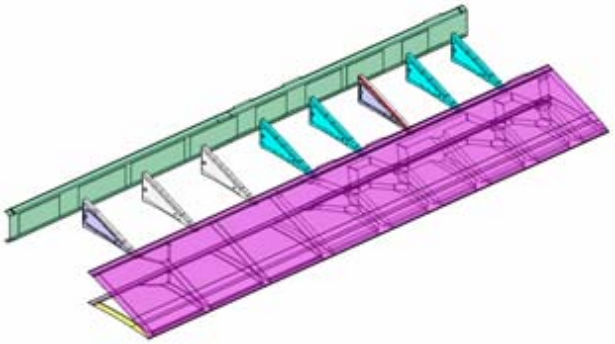

Figure 1. Flaperon exploded structure

These 10 components are made in composite and are connected by adhesive, in order to lighten aircraft frame. Adhesive thickness between the faced surfaces to connect should be as constant as possible in order to obtain a right structural connection. The influence of the tolerances applied to the 10 components on the value of the gap thickness at the interfaces between skin and rib, skin and spar, spar and rib has been deeply investigated by means of the proposed method. The free-form surfaces have been schematically represented by a set of control points, whose number and distribution have been opportunely designed. The industrial assembly sequence has been adopted for the analysis. The jigs commonly used to assembly the part of the flaperon involving aerodynamic surfaces have been considered in nominal conditions. The manufacturing process is assumed to produce parts whose dimensions and geometry are inside the tolerance ranges. The dimensions and the geometry of the considered components have been changed by means of a Monte Carlo simulation approach, though remaining inside their tolerance ranges, and the statistical distribution of the adhesive gap thickness has been estimated. To do this we have overcome the limits of CAT software to deal with free form surfaces. The estimated statistical distribution of the adhesive gaps thickness has been elaborated to obtain the trend of the thickness along the whole adhesive gap between each couple of faced surfaces. Monte Carlo simulation has been carried out by a well-known Computer Aided Tolerance software, eM-Tolmate of Tecnomatix®.
In the following we discuss the limits of the main approaches of the literature to the tolerance analysis; then, we present the case of study and the related problems of tolerance analysis. Finally, we show the adopted methods and the obtained results.

Tolerance analysis

The addition of the geometrical tolerances belonging to the assembly components is an unsolved problem. It is known as tolerance analysis. In literature different solutions to tolerance analysis exist, but all of them deal with the definition of schematic representations of the problem that are complex and far from the real problem (e.g. Refs 4 and 5).
The Direct Linearization Method (DLM) applies matrix algebra and root sum squares error analysis to vector loop based models to estimate tolerance stack-up assemblies (e.g. Refs 6-8). A tolerance is represented as a small variation of a vector. This method requires that datum and kinds of connections among the parts are specified.
The Variational solid modelling approach involves applying variations to a computer model of a part or assembly of parts (e.g. Refs 9-11). The surface, to which the tolerance is applied, is parameterized and divided in patches in the parametric space.
The kinematics approach to model stack-up functions finds its roots in robotic; matrices similar to the homogeneous coordinate transform matrices are used to determine the resulting tolerance zones (e.g. Refs 12-14). This method considers that a tolerance involves a small linear or angular displacement of a component as regards its nominal location, orientation and shape. The Proportioned Assembly Clearance Volume (PACV) method creates 3D-dimensional chains by using the Small Displacement Torsor (SDT) concept (e.g. Refs 15-17). SDT is used to express the relative position between two ideal surfaces.
However, these method are not easy to apply, especially for complex aerospace assemblies, since they were born to deal with elementary features, such as plane, hole, pin and so on. So the aid of computer is called for. In the recent years, the development of efficient and robust design tools has allowed to foresee manufacturing or assembly problems during the first steps of product modelling by adopting a concurrent engineering approach. Today Computer Aided Tolerance (CAT) software is readily available, but even if these tools provide

good results they have not been widely used (e.g. Refs 18-21). Commercial CATs are not completely true to the GD&T standards and need improvement after a better mathematical understanding of the geometric variations. The user needs expertise and great experience combined with a through understanding of the packages' theoretical base plus modelling principles to build a valid model and obtain relatively accurate results. Many are the questions without clear answers and without methods in place to deal with these questions: What are the functions of the product, how do we flow down these key product functions through into its detail parts? How to optimize the assembly process in order to reduce the tolerance impacts on these functions? Computer tools are not able to answer to these questions. Moreover, Computer Aided Tolerance software efficiently deals with mechanical assemblies where the feature to align are planes, hole-pin, but it hardly treats of free-form surfaces to connect.

Efforts to give answers to those questions were carried out in the aeronautic field. Sellakh proposed an assisted method for tolerance analysis of aircraft structures through assembly graphs and TTRS theory (e.g. Ref 22). Marguet presented a methodology to analyse and optimise the assembly sequence of simple shape assemblies (e.g. Refs 23 and 24). Ody showed a comparison among Error Budgeting techniques and 3D Tolerance Software Packages (e.g. Ref 25). Those papers present solutions of typical mechanical assemblies that involve the alignment of planes, holes and pins, but the aeronautic surfaces have a free form generally.

This paper shows a method to help the efficient and effective use of the current 3D tolerance analysis software packages to a specific and complex aircraft assembly.

Case of study

The case of study involves aerodynamic surfaces of flaperon. It develops two functions: the flap and the aleiron. Flap is an aerodynamic control surface that works in low speed condition when more lift is required; the increasing of lift is obtained by a consistent rotation of the flaperon, which changes the airfoil curvature by growing the lift surface. Aileron is an aerodynamic control surface, whose function is to roll the aircraft around its longitudinal axis; roll motion is obtained by alternatively moving flaperons with small rotation in high speed flight conditions.

It is constituted by 1 skin, 8 ribs and 1 spar (see Figure 1). Skin is the airfoil. Ribs are inserted in the skin whose shape they constrain. Spar closes the considered flaperon assembly and its function is to absorb axial and shear stresses applied to skin. These components are made up of composite material with carbon fibres and epoxy matrix in order to obtain a strength to weight ratio higher than metallic material's. The datum reference frame used to assembly all components is constituted by a spar plane (datum A), a chord plane (datum B) and a mating plane (datum C), as shown in Figure 2.

The 10 components are connected by adhesive. Adhesive thickness between the faced surfaces to connect should be as constant as possible in order to obtain an efficient structural connection and to avoid local compressions at the interface of faced surfaces due to strong reduction of thickness. The influence of the tolerances applied to the 10 components of the flaperon on the value of the gap thickness at the interfaces between skin and rib, skin and spar, spar and rib has been deeply investigated by means of the proposed method.

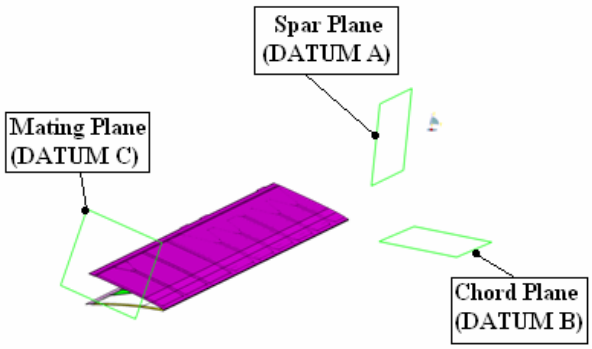

Figure 2. Flaperon datum reference frame

The dimensional and geometric tolerances applied to the 10 components of the flaperon are the following: the dimensional tolerance applied to the thickness and the profile tolerance on the aerodynamic surfaces of the skin (see Figure 3); the dimensional tolerance applied to the diameter of the rib's holes, the location tolerance applied to the rib's holes, the profile tolerance applied to the rib's surfaces that couple with the skin (see Figure 4); the dimensional tolerance applied to spar's thickness and the profile tolerance applied to spar's caps (see Figure 5). The location tolerances applied to the left and right holes of the rib in Figure 4 have the same value, but they are applied to holes with different values of nominal diameter.

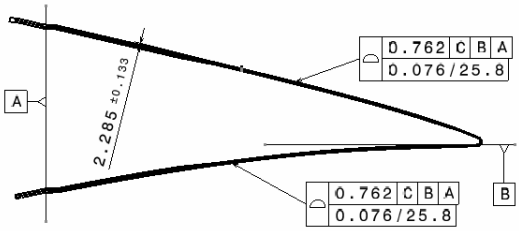

Figure 3. Tolerances applied to skin (datum C is the plane of the drawing)

Tolerance analysis for adhesive gaps: formulation

The 10 components of the flaperon at the three interfaces skin and rib, spar and rib, skin and spar are kept together by adhesive without rivets.

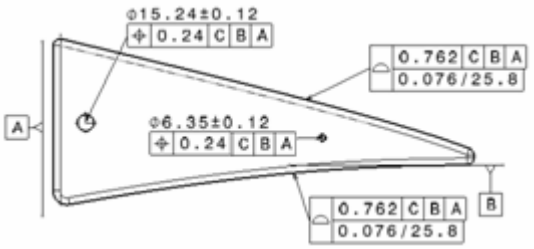

Figure 4. Tolerances applied to a rib (datum C is the plane of the drawing)

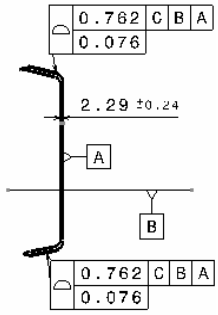

Figure 5. Tolerances applied to spar (datum C is the plane of the drawing)

Adhesive thickness between the faced surfaces to connect should be as constant as possible to guarantee an efficient structural connection. In the same time the thickness of the adhesive gap has to avoid local compressions at the interface of faced surfaces due to strong reduction of thickness.
The present work has estimated the probability that interferences and uniformity of the gap occur at the interfaces between skin and rib, spar and rib, skin and spar. A net is laid between the faced surfaces to stick in order to maintain the adhesive inside the gap. An interference occurs if the distance between the two faced surfaces is shorter than the minimum thickness the net achieves when it is squeezed between the faced surfaces (d_{min}=0.08 mm, see Figure 6). Adhesive gap between two faced surfaces is considered uniform if the difference between the maximum and the minimum values of the thickness along the gap is lower than a reference value (0.3 mm), as shown in Figure 7.

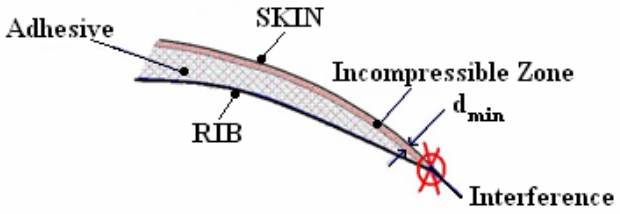

Figure 6. Interference between skin and rib

The presence of interferences and the uniformity of each gap thickness have been estimated for five gaps, S1-S5 in Figure 8.

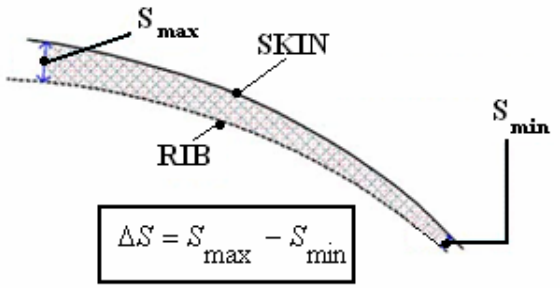

Figure 7. No uniform adhesive thickness between skin and rib

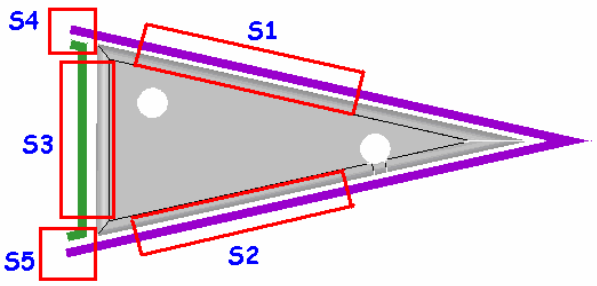

Figure 8. Scheme of the considered adhesive gaps

Moreover, the trend of the gap thickness among flaperon's components, that has to be filled with adhesive, has been evaluated too.
The trend of the gap thickness is influenced by the small deviations from nominal that each component of the flaperon has due to the applied tolerances (indicated as T in the following) and to the assembly sequence by jigs (called A in the following).
The industrial assembly sequence of the considered flaperon part is constituted by three steps. The first step involves the insertion of the skin into its assembly jig to constitute a sub-assembly (see Figure 9). During the second step each rib is coupled with its assembly jig and, then, it is mated with the previous obtained sub-assembly, as shown in Figure 10. The gaps among skin and ribs are filled with adhesive and fixed at 180°C. Then, the jigs of the ribs are removed and the spar is located on the ribs (see Figure 11). The gaps among skin, ribs and spar are filled with adhesive at room temperature.
The adopted process manufactures skins whose thickness varies inside a dimensional tolerance range (that is called T1). These thickness variations may increase or decrease the nominal thickness of the gap between skin inner surfaces and rib, since skin mates the used jig along its outer surfaces. Moreover, the manufacturing process may vary the shape and location of skin outer surfaces inside a profile tolerance range. This involves a variation of the angle between the upper and lower surfaces of

the skin that may decrease or increase as regards the nominal value.

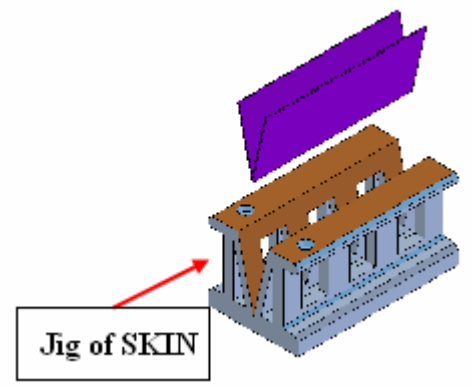

Figure 9. Scheme of the insertion of the skin into its assembly jig

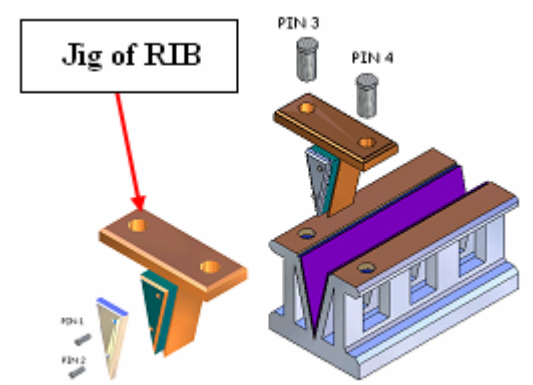

Figure 10. Scheme of the coupling of a rib with the skin

Generally, the adopted process manufactures skins with a value of the angle between the upper and lower surfaces equal to nominal or greater than the nominal one, while seldom the angle has a value lower than nominal.
Therefore, when the skin is assembled and it is different by nominal, it is forced to mate its jig, due to the flexibility of the composite, but it does not try to mate the jig up to the end vertex. The skin arrives up to a distance of 0.24 mm from the vertex of the jig. The position of the skin as regards its jig has been indicated as A1 in the following and it may assume only two value (0 and 0.24 mm).
A rib is generally produced with its bounding surfaces ranging inside the profile tolerance ranges (called T2 and T3 in Figure 12b). It may rotate as regards its jig during assembly due to the changes in holes position inside a location tolerance range (called A2 in Figure 12b).
The spar is generally manufactured with a thickness ranging inside a dimensional tolerance range (T4 in Figure 13). Its caps may vary their shape and location inside a profile tolerance range. This involves a variation in caps inclination as regards the nominal values (called T5 and T6 in Figure 13).

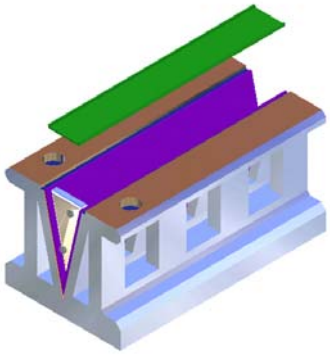

Figure 11. Scheme of spar positioning

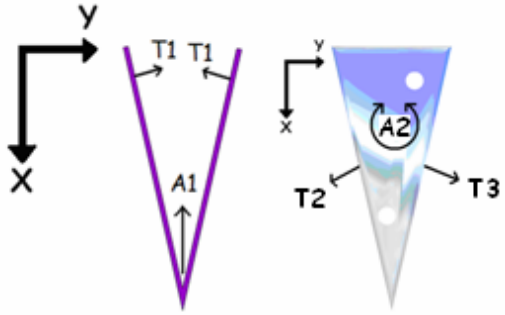

Figure 12. a)Skin deviations from nominal: T1 and A1; b) Rib deviations from nominal: T2, T3 and A2

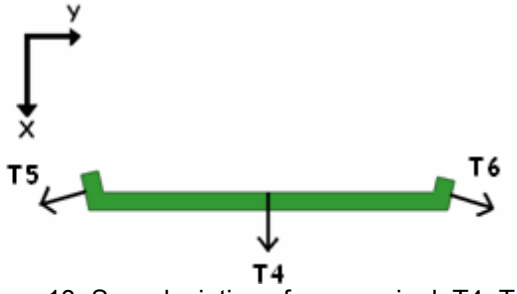

Figure 13. Spar deviations from nominal: T4, T5 and, T6.

The applied tolerances T2, T3, T4, T5 and T6 and the assembly constraint due to rib holes location tolerance A2 have been considered distributed according to a Gaussian probability density function. The assembly constraint A1 may assume only the two values that actually present during assembling, as previously described. The dimensional tolerances applied to skin and spar thickness (T1 and T4) have been considered to assume only two values, the nominal and the maximum allowable by the applied tolerances, since those two conditions are commonly obtained by the actual manufacturing processes.
Monte Carlo simulation has been adopted to define the probability distribution of the distance between the faced surfaces belonging to each gap. The number of runs of simulation has been fixed at 50000, once some tests have proved that 50000

guarantees a reliable estimation of the mean and the standard deviation of the distance probability distribution characterising each gap.
Finally, a sensitivity analysis has been carried out in order to identify the variables (tolerances or assembly constraints distributed as a Gaussian probability density function) mainly affecting the thickness of each gap. The weight of each variable has been calculated by evaluating the variance of the thickness σ_{TOT}, when all the previously introduced variables are applied to flaperon's components, and the variance of the thickness σ_{TOT-Ti}, once i-th variable is not applied to the flaperon's components:

$$W_i = \frac{\sigma^2_{TOT} - \sigma^2_{TOT-Ti}}{\sigma^2_{TOT}} \cdot 100 \quad (1)$$

Tolerance analysis for adhesive gaps: proposed method

The aim of the tolerance analysis, that has been carried out in this work, is to obtain a map of the distance between the two faced surfaces, along the whole gap, since the critical zones of flaperon's airfoils need to be identified. In fact, the two faced surfaces have an unknown free form that do not allow us to focus the attention only on the surface vertices. CAT software performs a surface to surface distance by taking into account the barycentres of the two faced surfaces. This limit has been overcome by drawing control points on each surface. The pattern of control points has been placed along a profile in the middle of the considered surface, as shown in Figure 14, since the 3D model of the considered flaperon's components is obtained as the extrusion of a 2D section characterised by free form profiles.
For example, if we consider the gap between skin and rib, a pattern of points may be modelled on rib nominal surface, as shown in Figure 14. A normal vector is associated to each point of the rib; it is perpendicular to skin's nominal profile too. So rib's pattern of normal vectors intersect the nominal profile of skin by defining another pattern of points. To evaluate the distribution of the distance between skin and rib, when rib and skin have small deviations from the nominal inside the applied tolerance ranges, the minimum distance of each point of the rib from the skin surface need to be calculated. CAT software calculates a point to point distance between the two defined patterns that does not correspond to the minimum distance between the two corresponding surfaces. The minimum distance among the two surfaces has been calculated by projecting the point to point distance on the vector perpendicular to the nominal surfaces of the rib and the skin. The obtained values of distance are very near to the minimum ones, as demonstrated in the following.

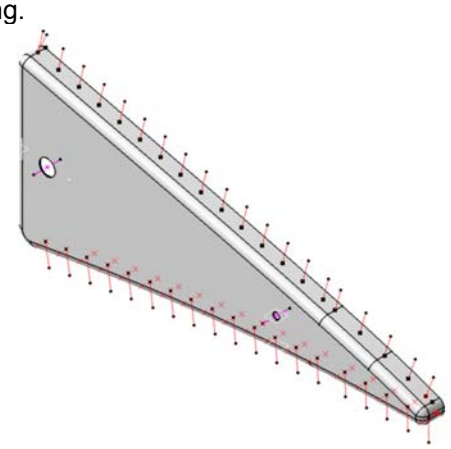

Figure 14. Control points on rib's surfaces faced to skin (S1 and S2 gaps)

Consider **A** point on rib nominal profile in Figure 15. This point is aligned with **B** of skin nominal profile (i.e. **A** and **B** are on the unit vector $\mathbf{n_A}$ that is perpendicular to rib nominal profile in **A)** and the minimum distance between skin and rib profiles is **AB**. The tolerances and the assembly sequence applied to rib and skin affect their location and orientation. In fact, **A** and **B** points move to **A'** and **B'** points that lie on skin and rib surfaces to which tolerances and assembly constraints are applied (called SKIN_A1/T1 and RIB_A2/T2/T3 in Figure 15). The minimum distance becomes **A'B**", where **B"** is the intersection of the unit vector perpendicular to the rib profile in **A'** point, $n_{A'}$, with skin profile. The distance **A'B"** may not be calculated by the CAT software. The software calculates automatically the distance **A'B'**. We set the software to calculate $\mathbf{A'B'_p}$ distance, where $\mathbf{B'_p}$ is the projection of **B'** on the unit vectors $\mathbf{n_A}$.
We draw the tangent line to skin profile in **B"** point that intersects the line connecting $\mathbf{B'B'_p}$ in **C** point. **K** point is due to the intersection of the unit vector perpendicular to the rib nominal profile in **A'** point, $\mathbf{n_A}$, with skin profile. **D** point is obtained by intersecting the line connecting **B'** and $\mathbf{B'_p}$ with the unit vector $\mathbf{n_{A'}}$.
The distance $A'K = \frac{A'B''}{cos\,\vartheta}$ since **A'KB"** is a right-angle triangle in **B"**. The θ angle between $\mathbf{n_A}$ and $\mathbf{n'_A}$ assumes 0.5° as maximum values for the chosen pattern of points on rib surface. Therefore, $\cos\theta \approx 0.999996$ and $\mathbf{A'K \cong A'B''}$.
The **CB"D** triangle is a right-angle triangle in **B"** and the angle $\hat{C}$ is equal to θ, since it is included between two lines that are perpendicular to $\mathbf{n_A}$ and $\mathbf{n'_A}$ respectively.

The distance $CB'' = \frac{CD}{\cos\vartheta}$ and **CB"≅CD,** since cosθ≈0.999996.
Therefore, the two triangles **A'KB"** and **CB"D** are right-angle and isosceles that may happen only if the two triangles degenerate in the segments **A'K=A'B"** and **CD=CB"**. Therefore, **DB"** and **KB'$_p$** have a negligible lenght if compared to **A'B"**, so **A'B'$_p$≅AK≅A'B"**. Therefore, the calculated distance **A'B'$_p$** may be considered to coincide with the actual distance **A'B"**.
The same considerations have been applied to choose the pattern of control points belonging to the couples of faced surfaces along skin and spar, rib and spar interfaces. The results are shown in Figure 16 and 17.

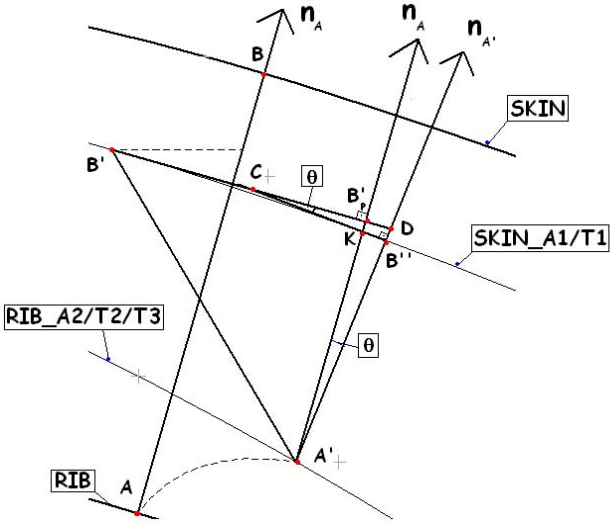

Figure 15. Scheme to calculate the minimum distance in **A** and **C** points

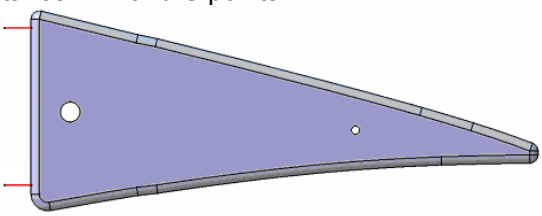
Figure 16. Control points on rib's surface faced to spar (S3 gap)

Finally, few comments on profile tolerances applied to rib and spar need to clarify the simulations we have carried out. A profile tolerance of 0.762 mm is applied to the bounding surfaces of rib and spar: it means that each of these surfaces should be included between two offset surfaces that are symmetrically placed as regards the nominal one and at a distance of 0.762/2 mm from it. This tolerance controls the location, the orientation and the shape of rib and spar surfaces.

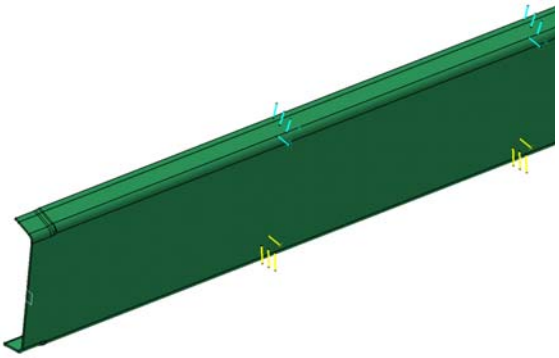
Figure 17. Control points on spar's surfaces faced to rib (S3) and to skin (S4 and S5 gaps)

Moreover, a smaller profile tolerance of 0.076 mm is applied to any part of the profile of 25.4 mm length belonging to the surface. It controls only the shape c, rib and spar profiles, since no datum reference frame is used. This profile tolerance may not be dealt with the CAT software, since it does not belong to the standards, such as ISO 1101 or ASME 19.4Y. Therefore, we have applied this smaller profile tolerance of 0.076 mm to the whole profile of spar and rib surfaces by adopting a more conservative point of view. The further applied dimensional and geometrical tolerances have been simulated according with standards.

Tolerance analysis for adhesive gaps: results discussion

The distribution of the calculated distance between any couple of considered points of the patterns looks like to a Gaussian, whose parameters (mean and standard deviation) have been estimated. The more probable values of the distance are included inside the range ±3σ centred around the mean, i.e. 99.73% of the distribution.
Figure 18 shows the ranges including 99.73% of the distribution of the calculated distance of each couple of points characterising S1 gap, when A1 and T1 have the maximum deviation from the nominal (called worst case). Figure 19 shows the ranges of S1 gap, when A1 and T1 assume nominal values (called nominal case).
We can note that the mean value of gap thickness of 0.25 mm in nominal conditions reduces to 0.05 mm when spar moves from the nominal. The variance of the obtained values of the calculated distance seems to keep similar from nominal to worst cases. The gap thickness of the worst case may assume negative values lower than those due to nominal case; this involves a percentage of assemblies with interferences greater than in the nominal case.

Table 1. Maximum value of the percentage of assemblies with interferences and with a no-uniform gap

	Interferences [%]		
Adhesive gaps	**Nominal case**	**Worst case**	**No uniform gap [%]**
S1	4	68	3
S2	4	50	4
S3	0	99	0
S4	4	80	4
S5	4	70	4

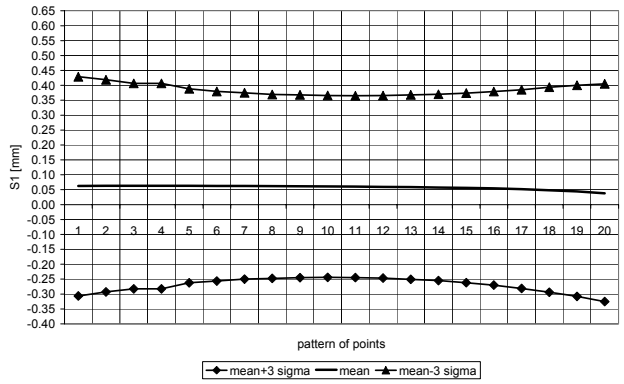

Figure 18. Ranges including 99.73% of the distributions of the distance of all the couples of points of S1 gap: worst case

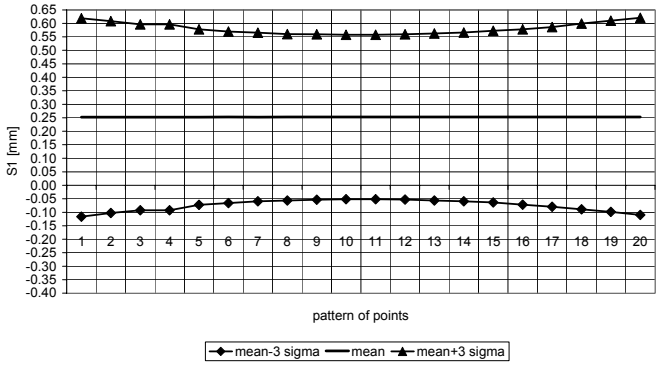

Figure 19. Ranges including 99.73% of the distributions of the distance of all the couples of points of S1 gap: nominal case

The percentage of assemblies with interferences has been estimated by calculating the area under the obtained Gaussian distribution below the admitted limit of 0.08 mm (see Table 1). As noted before, it is very low in nominal conditions, but it increases considerably for the worst case.
The same considerations may be repeated for S2 gap when spar and rib move from nominal conditions (see Figures 20 and 21) or for S3, S4 and S5 gaps when spar, skin and rib move from nominal conditions (see Figures 22-27). The differences between S1 and S2 gaps are due to the different profiles of the upper and lower free form surfaces of rib and skin; the same is for S4 and S5 gaps.

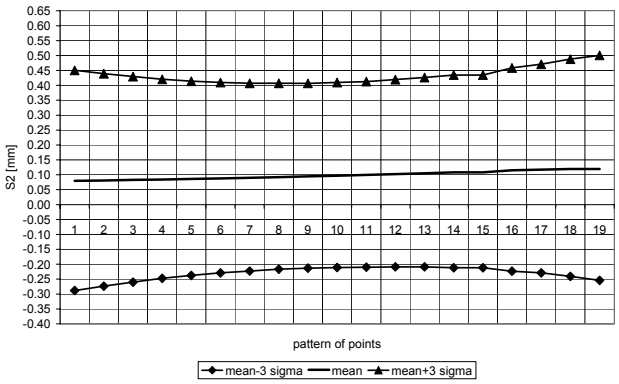

Figure 20. Ranges including 99.73% of the distributions of the distance of all the couples of points of S2 gap: worst case

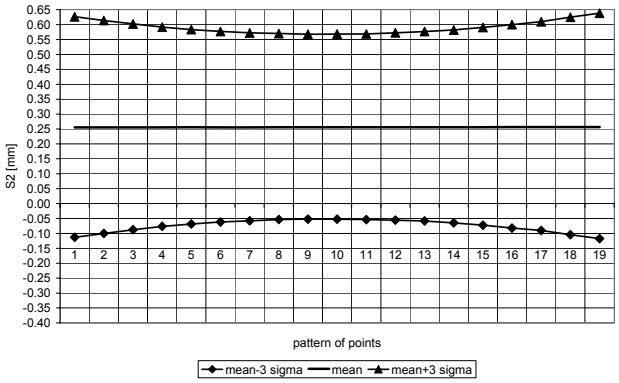

Figure 21. Ranges including 99.73% of the distributions of the distance of all the couples of points of S2 gap: nominal case

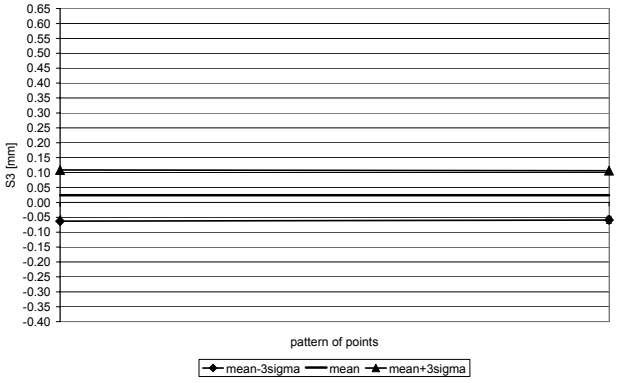

Figure 22. Ranges including 99.73% of the distributions of the distance of all the couples of points of S3 gap: worst case

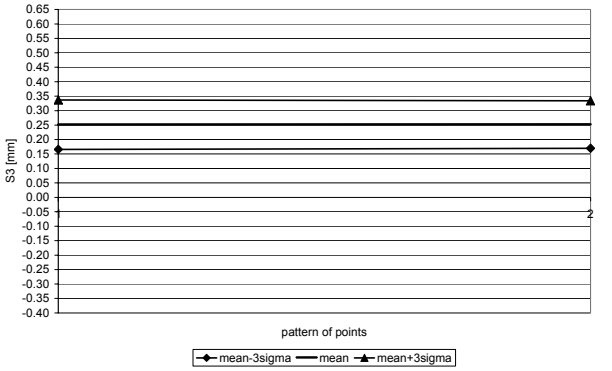

Figure 23. Ranges including 99.73% of the distributions of the distance of all the couples of points of S3 gap: nominal case

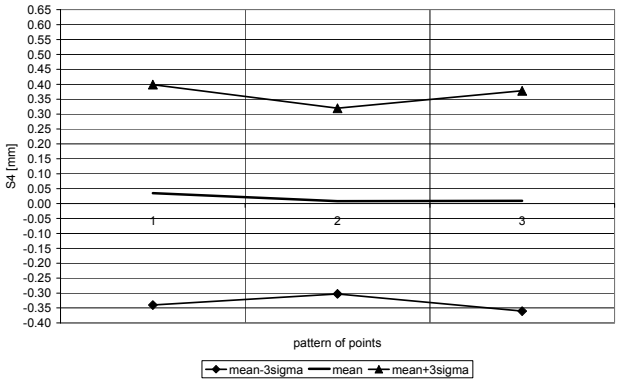

Figure 24. Ranges including 99.73% of the distributions of the distance of all the couples of points of S4 gap: worst case

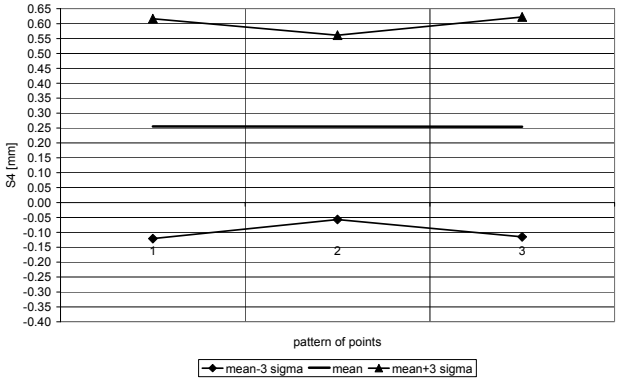

Figure 25. Ranges including 99.73% of the distributions of the distance of all the couples of points of S4 gap: nominal case

To estimate the uniformity of the gap between two faced surfaces the distribution of the difference (ΔS) between the maximum and the minimum values of the calculated distances has been estimated. The percentage of parts whose ΔS overcomes the fixed maximum value (0.3 mm) has been evaluated and shown in Table 1. The percentage of parts with a no-uniform gap is always very low.

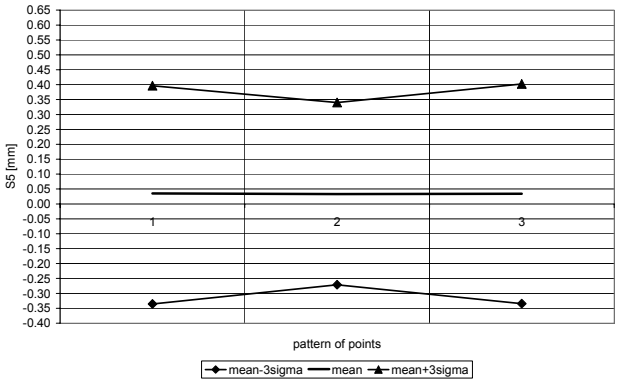

Figure 26. Ranges including 99.73% of the distributions of the distance of all the couples of points of S5 gap: worst case

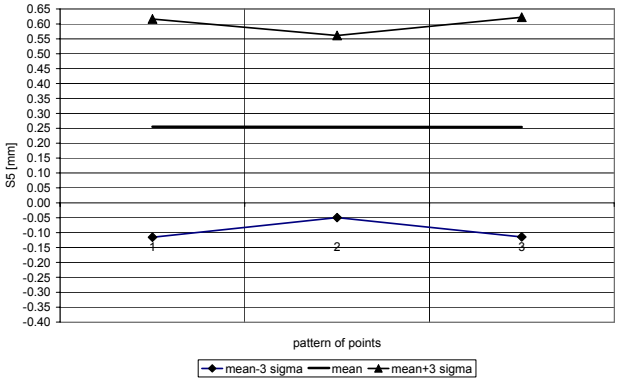

Figure 27. Ranges including 99.73% of the distributions of the distance of all the couples of points of S5 gap: nominal case

All the obtained results has found confirmation in the actual assembly process data.

The results of the sensitivity analysis on the adhesive gaps thickness is shown in Figure 28. We can observe that the gaps between the rib and the skin (called S1 and S2) are significantly affected by the profile tolerance (weight of 70%) and location tolerance of the rib holes (weight of 30%). The profile tolerance has a weight greater than that of location tolerance, since the range of profile tolerance is greater than the range of location tolerance. The gap between the rib and the spar is interested by the location tolerance applied to the two holes of the rib (weight of 100%): the left hole has an effect greater than the right one. This is due to the fact that when the location tolerance of the left hole is simulated, the location tolerance of the right hole is not considered (together with the other applied tolerances) and, therefore, the rib rotates around the right hole. The distance of the considered points of the rib, that are faced to spar, from the rotation centre (i.e. right hole centre) is longer than that from the left hole. Therefore, the deviations of rib points faced to spar from nominal,

due to the rotation around the right hole, are greater than that due to the rotation around the left hole. The gaps between spar and skin are interested by the profile tolerances applied to the spar's caps.

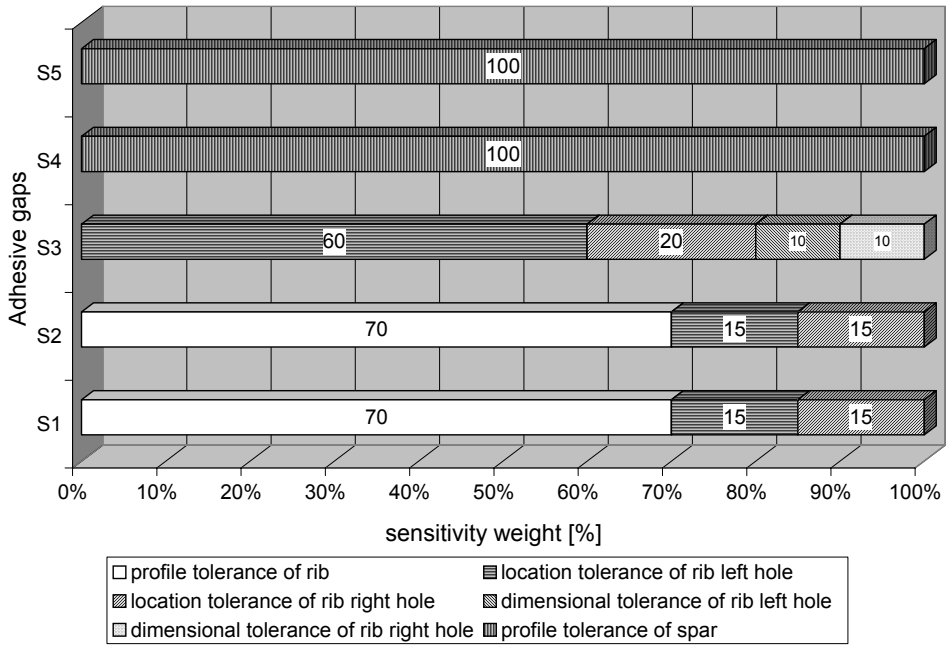

Figure 28. Results of sensibility analysis on adhesive gaps

Tolerance analysis of rib profile

Afterwards, the analysis has focused the attention on the profile tolerance applied to rib's bounding surfaces. It aims to verify if the small deviation of the rib location and orientation from the nominal, due to the location tolerances applied to the rib's holes, make the rib's bounding surfaces to move out the profile tolerance range. This interest was born by the influence of the rib location tolerance on S1 and S2 gaps we found before.

The two surfaces of the rib to which the profile tolerance is applied have been considered. They have been offset of half of the profile tolerance range both outside and inside the rib to obtain two bounds for each surface.

Figure 29 shows the offsetting of the two surfaces outside the rib. The curvature of each bound has been compared with that of the corresponding rib nominal surface in order to evaluate the agreement with the rib one. Figure 30 shows the analysis of the curvature of one bound and of the corresponding rib upper surface.

The calculated maximum difference of curvature is very low ($6.1\ 10^{-4}\ mm^{-1}$).

Monte Carlo simulation has been adopted to define the probability distribution of the distance between rib surfaces and bounds. The location tolerance applied to rib's holes is the unique simulated tolerance.

The location tolerance applied to rib's holes changes the length and the orientation of the wheel-base between holes as regards the nominal one that is shown in Figure 31. The assembly of rib with its jig provides for aligning a hole of the rib with a pin of the jig and coupling them. Then, the rib is rotated around the centre of the coupled hole-pin up to insert the second pin of the jig in the second hole of the rib (i.e. up to align the wheel-bases of rib and jig), as shown in Figure 32. The rotation may happen around any point of rib wheel-base, if the two centres of the holes are placed in opposite directions as regards the nominal wheel-base. The size of the rotation is as much as the centres of the holes deviate from the nominal inside the location tolerance.

The points of the rib's surfaces, to which the profile tolerance is applied, that have the greatest deviation from the nominal due to rib rotation are the extremes, since they have the greatest distance from the centre of rotation. Therefore, the control points used for Monte Carlo simulation are the two extreme points of each rib profile.

The distance between rib surface and bounds has been evaluated for each couple of extreme points.

The results show how the small deviations of the rib from the nominal due to the location tolerance applied to the holes, that involves small rotations and translations of the rib as regards its nominal

position, keep rib's surfaces always inside the profile tolerance range.

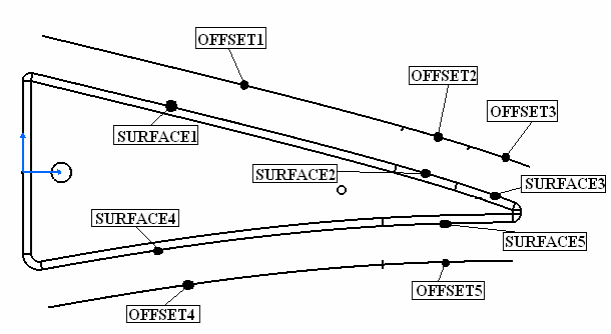

Figure 29. Offsetting of rib's surfaces

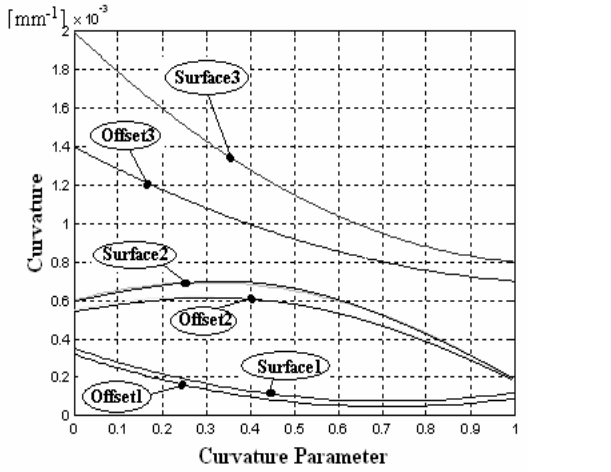

Figure 30. Curvature of rib upper surface and the corresponding bound

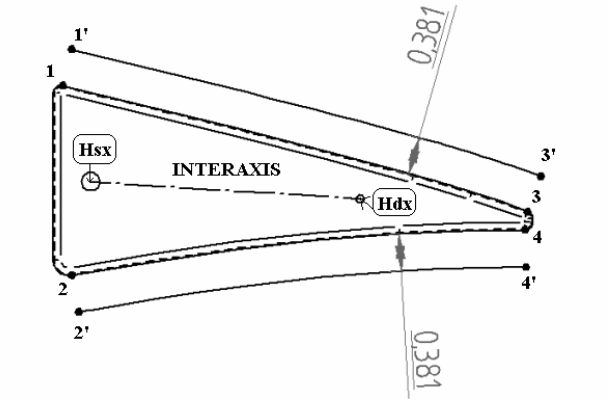

Figure 31. Centres of rib holes in the same direction

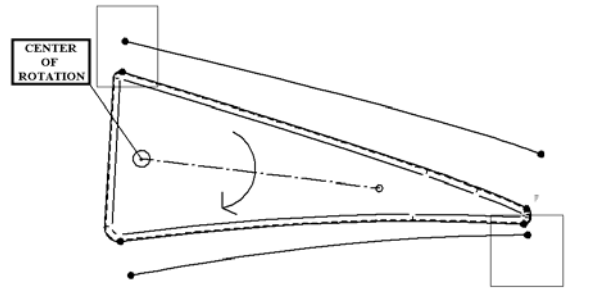

Figure 32. Centres of rib holes in opposite directions

Conclusions.

The present work shows an original method to deal with tolerance analysis involving free form surfaces in composite material.
The proposed method has been applied to the part of the flaperon involving aerodynamic surfaces in order to verify its structural integrity. It has allowed to evaluate if the thickness of the gap between each couple of faced surfaces were uniform, i.e. the difference between the maximum and the minimum values of the thickness along the gap were lower or equal to 0.3 mm. In the same time it has allowed to verify if the thickness of the gap were greater than 0.08 mm in order to avoid interferences among the coupled surfaces.
A pattern of control points has been opportunely placed on each free form surface. The pattern of control points has been used to identify that the gap is uniform even if the percentage of interferences strongly increases when the components move from nominal. Moreover, a sensitivity analysis has been carried out in order to identify the tolerances that mostly affect the thickness of adhesive gaps.
The proposed method may be used to evaluate the aerodynamic requirements of flaperon too. It is current matter of further studies.
The proposed method may be used to assist the designer to verify the functional performances of a complex shape assembly. In the same time this method may help to choose among alternative assembly sequences by evaluating if they allow the assembly to achieve the functional requirements. Further studies are proceeding along this direction. The developed method is complementary to the current 3D tolerance analysis software packages, such as eM-Tolmate, since it is able to deal with the specificity and the complexity of an aircraft assembly.

Acknowledgements

The authors are grateful to AGUSTA Westland at Anagni for funding and supporting this work. A special thanks to Mr Franco Natalizia.

References

1 Parkinson A., Chase K., Rogers M., Robust design via tolerance analysis in the design stage, Proc. of ASME Design Engineering Technical Conferences, 1999, Las Vegas, Nevada, Paper # DETC99/DAC-8577.
2 Whitney D. E., Mechanical assemblies. Their design, manufacture and role in production development, Oxford University Press Inc., 2004.

3 Delchambre A., CAD method for industrial assembly. Concurrent Design of product, equipment and control systems, John Wiley & Sons Ltd, 1996.
4 Hong Y.S., Chang T.C., A comprehensive review of tolerancing research, Int. J. Prod. Res., 2002, vol. 40, no. 11, pp. 2425-2459.
5 Shen Z., Ameta G., Shah J.J., Davidson J.K., A comparative study of tolerance analysis methods, Proc. of ASME 2004 Design Engineering Technical Conferences and Computers and Information in Engineering Conference, Salt Lake City, Utah, 2004, Paper #DETC2004-57699.
6 Chase K.W., Gao J., Magleby S.P., Tolerance analysis of 2- and 3-D Mechanical Assemblies with Small Kinematic Adjustments, Advanced Tolerancing Techniques, John Wiley, 1997, Ed. by H.C. Zhang, Chap. 5, pp. 103-137.
7 Gao J., Chase K.W., Magleby S.P., Comparison of assembly tolerance analysis by the Direct Linearization and Modified Monte Carlo Simulation methods, Proc. of ASME Design Engineering Tech. Conf., 1995, pp. 353-360.
8 Chase K.W., Multi-Dimensional Tolerance Analysis (Automated Method), Dimensioning and Tolerancing Handbook, P. jr. Drake, McGraw-Hill, Chapter 13.
9 Gupta S., Turner J.U., Variational solid modeling for Tolerance Analysis, IEEE Computer Graphics & Applications, May 1993, pp. 64-74.
10 Whitney D.E., Mantripraga R., Adams J.D., Rhee S.J., Toward a theory for design of kinematically constrained mechanical assemblies, The Int. J. of Robotics Research, vol. 18, 1999, pp. 1235-1248.
11 Li B., Roy U., Relative positioning of toleranced polyhedral parts in an assembly, IIE Transactions, 2001, vol. 33, pp. 323-336.
12 Laperrière L., Lafond P., Modeling tolerances and dispersions of mechanical assemblies using virtual joints, Proc. of ASME Design Engineering Technical Conferences, 1999, Las Vegas, Nevada, Paper #DETC99/DAC-8702.
13 Laperrière L., Lafond P., Jacobian-based Modeling of Dispersions Affecting Pre-Defined Functional Requirements of Mechanical Assemblies, Proc. of IEEE Int. Symposium on Assembly and Task Planning, 1999, pp. 20-25.
14 Laperrière L., Kabore T., Monte Carlo simulation of tolerance synthesis equations, Int. J. Prod. Res., vol. 39, 2001, pp. 2395-2406.
15 Teissandier D., Couetard Y., Gerard A., A computer aided tolerancing model: proportioned assembly clearance volume, Computer-Aided Design, vol. 31, 1999, pp. 805-817.
16 Bourdet P., Mathieu L., Lartigue C., Ballu A., The concept of the small displacement torsor in metrology, Int. Euroconference, Advanced Mathematical Tools in Metrology, Oxford, 1995.
17 Clément A., Rivière A., Serré P., Valade C., The TTRSs: 13 Constraints for Dimensioning and Tolerancing, Geometric Design Tolerancing: Theories, Standards and Applications, ElMaraghy H.A. (Ed.), Chapman & Hall, 1998, pp. 123-131.
18 Turner J., Gangoiti A.B., Tolerance Analysis Approaches in commercial software, Concurrent Engineering, vol. ½, 1991, pp. 11-23.
19 Chase K.W., Magleby S.P., Glancy C.G., A compressive system for Computer-Aided Tolerance Analysis of 2-D and 3-D Mechanical Assemblies, Proc. of the 5th Int. CIRP Seminar on Computer-Aided Tolerancing, Toronto, Canada, 1997.
20 Salomons O.W., van Houten F.J.A.M., Kals H.J.J., Current status of CAT Systems, Geometric Design Tolerancing: Theories, Standards and Applications, H.A. ElMaraghy ed., Chapman & Hall, London, 1998, pp. 438-452.
21 Prisco U., Giorleo G., Overview of Current CAT Systems, Integrated Computer Aided Engineering 2002; vol. 9 (4), pp. 373-387.
22 Sellakh R., Rivière A., Chevassus N., Falgarone H., An assisted method for tolerancing applied to aircraft structures,Proc. of 8th CIRP Int. Seminar on Computer Aided Tolerancing, Charlotte, North Carolina, 2003, pp. 187-198.
23 Marguet B., Mathieu L., Tolerancing problems for aircraft industries, Proc. of CIRP Int. Seminar on Computer Aided Tolerancing, Geometric Design Tolerancing: Theories, Standards and Applications, ElMaraghy H.A. (Ed.), Chapman & Hall, 1998, pp. 419-427.
24 Marguet B., Mathieu L., Aircraft Assembly analysis method taking into account part geometric variations, Global Consistency of Tolerances, Van Houten F. and Kals H. (Eds.), Kluwer Academic Publishers, 1999, pp. 365-374.
25 Ody R., Burley G., Naing S., Corbett J., Geometric and Dimensioning Tolerances in error budgeting for assembly-centric design of aerostructures, 7th CIRP Int. Seminar on Computer Aided Tolerancing, ENS de Cachan, France, 2001, pp. 111-120.